Vol. 90: 23–39, 2024 https://doi.org/10.3354/ame02006

AQUATIC MICROBIAL ECOLOGY Aquat Microb Ecol

Published February 29



Determining growth rates of heterotrophic bacteria from 16S rRNA gene sequence-based analyses of dilution experiments

Michael R. Landry^{1,*}, Alexandra L. Freibott¹, Ariel Rabines^{1,2}, Andrew E. Allen^{1,2}

¹Scripps Institution of Oceanography, University of California San Diego, La Jolla, CA 92093, USA ²Microbial and Environmental Genomics, J. Craig Venter Institute, La Jolla, CA 92037, USA

ABSTRACT: Vital rates, including growth responses to environmental variability, are poorly characterized for the diverse taxa of heterotrophic bacteria (HBact) in marine ecosystems. Here, we evaluated the potential for combining molecular analyses with dilution experiments to assess taxon-specific growth (cell division) and net growth rates of HBact in natural waters. Two-treatment dilution experiments were conducted with in situ incubations under 3 environmental conditions in the California Current Ecosystem, at offshore and inshore sites during a warm upwellingsuppressed year (2014) and for normal inshore upwelling, representing a 33-fold primary production range. Relative sequence reads from 16S rRNA metabarcoding were normalized to total HBact counts from flow cytometry for community abundance and rate calculations. Composition varied from dominance of Alphaproteobacteria (56%) in oligotrophic offshore (SAR11) and mesotrophic inshore waters (SAR11 and Rhodobacteria) to Bacteriodes/Flavobacteria dominance (64%) and mixed sub-taxon importance (Polaribacter, Rhodobacteria, Formosa) during upwelling. Net growth rates in bottles, validated by comparison to ambient community net growth following a satellitetracked drifter, varied from near steady state for offshore and inshore conditions to dynamic community changes during upwelling. Mean growth rates doubled (0.33 to $0.62~\text{d}^{-1}$) over the productivity range, and taxon estimates varied from $-0.17 \,\mathrm{d}^{-1}$ (Formosa, offshore) to 1.53 d⁻¹ (SAR11, upwelling). Increasing growth of Flavobacteria and Rhodobacteria paralleled their abundance and dominance increases with productivity. SAR11 growth remained higher than average with increasing production, despite declining abundances. We highlight possible PCR or 16S rRNA gene copy biases of growth rate estimates as research needs for further applications of this approach.

KEY WORDS: Heterotrophic bacteria · Net growth rate · Growth rate

- Resale or republication not permitted without written consent of the publisher

1. INTRODUCTION

Heterotrophic bacteria (HBact) play major roles in ocean food webs, carbon cycling, organic matter degradation and biogeochemical transformations, but how these functions relate to variability in taxonomic composition and population activity remains poorly known due to large uncertainties in key vital rates, such as growth, that underly population responses to environmental variability. For instance, slow growth,

on the order of $0.1~\rm d^{-1}$, has long been the accepted paradigm for HBact in the central oceans (Kirchman 2016). However, mean growth rate estimates ($\sim 0.80~\rm d^{-1}$) from bacterial phospholipid turnover in the subtropical Atlantic and Pacific are many times higher (Popendorf et al. 2020). Such rate uncertainties are amplified among taxonomic groups, locations and varying ecological conditions (Fuchs et al. 2000, Yokokawa et al. 2004, Teira et al. 2009, Ferrera et al. 2011, Sánchez et al. 2017, Fecskeová et al. 2021).

While novel approaches such as 16S rRNA:rDNA ratios have been used to infer higher- or lower-thanaverage growth rates among HBact taxa in naturally collected water samples (Campbell et al. 2011), most taxon-specific growth estimates come from manipulation experiments. A common approach is to determine the rates of cell increase over several days in ~1-µm filtered water from which grazers (and most phytoplankton) have been removed, using fluorescent in situ hybridization (FISH) techniques to distinquish rates of select populations, generally in comparison to unfiltered controls (Ferrera et al. 2011, Sánchez et al. 2017, 2020, Fecskeová et al. 2021). Variations on that theme include multi-day grow-out experiments in which samples are highly diluted with 0.2- μm filtered water or combinations of filtration and dilution (e.g. Fuchs et al. 2000, Yokokawa et al. 2004, Yokokawa & Nagata 2005) to both decrease grazing and reduce competition for dissolved organics. We refer here to such manipulations as dilution cultures, analogous to the approach for calibrating ³H-leucine uptake rates (Kirchman & Ducklow 1993, Alonso-Sáez et al. 2010), but different from typical Landry-Hassett dilution experiments that run for shorter periods (24 h) with natural seawater controls (Landry & Hassett 1982) and are generally less extreme perturbations of the coupled production-grazingremineralization relationships within microbial communities (Landry 1993). While variations of the latter have been used extensively to quantify growth rates of phytoplankton (phototrophs, including cyanobacteria) (e.g. Landry et al. 2008, 2011, 2022), the approach has been sparsely applied to studies that look to resolve growth rates among HBact taxa (e.g. 2 experiments by Yokokawa & Nagata 2005). It is also the case that although DNA sequencing might benefit such studies by reducing the time and costs of population analyses and extending consideration to a greater diversity of taxa, these studies require careful use of standards (Fecskeová et al. 2021) or other normalization protocols to apply their relative read abundances to methods that need quantitative abundance data for rate calculations.

In the present study, we examined the potential for determining taxon-specific growth rates of HBact from dilution experiments using flow cytometric abundances as the quantitative basis for apportioning relative sequence abundances among individual groups. To evaluate methodology, we examined bacterial community composition and growth rates over offshore, inshore and interannual differences that span the broad range of natural productivity variability in the California Current Ecosystem (CCE). Using

drifter arrays to follow water patches and as a platform for *in situ* incubations under natural conditions of light and temperature, we also uniquely validated net growth rates measured in incubation bottles relative to net growth rates observed in the ambient water column.

2. MATERIALS AND METHODS

2.1. Study sites and experiments

We determined taxon-specific abundances and growth rates of HBact for 3 environmental scenarios that span the broad range of CCE conditions. The main data contribution was from cruise P1408, which sampled the system at 3 inshore and 2 offshore locations in August 2014 (sites 1–3 and 4–5, respectively, in Fig. 1) during a period of anomalously high seasurface temperature and low upwelling (Bond et al. 2015, Kintisch 2015, Jacox et al. 2016, Kahru et al. 2018). To contrast with these low productivity conditions, we analyzed additional experiments from cruises P0605 (May 2006) and P0704 (April 2007) with high upwelling and productivity in the same vicinity as the P1408 inshore sites (Fig. 1).

Cruise sampling and experiments were done in coordinated quasi-Lagrangian studies that used a satellite-tracked free-drifting array with a 3-m droque centered at 15 m to follow selected water parcels for 3-5 d (Landry et al. 2009). For each experiment, seawater was collected from Niskin bottles on earlymorning conductivity—temperature—depth (CTD) hydrocasts (~02:00 h local time) in close proximity (~100 m) to the drifter position. For each depth, we prepared a 2-treatment dilution experiment (Landry et al. 2008, 2011), with one polycarbonate bottle (2.7 l) containing unfiltered seawater (100%) and the second (diluted) bottle consisting of ~33% whole seawater with filtered water from the same depth. Seawater was filtered directly from the Niskin bottles using a peristaltic pump, silicone tubing and in-line 0.1-µm Suporcap filter capsules that had previously been acid washed. Dilution bottles were first given a measured volume of filtered water and then filled gently to the top with unscreened water from the Niskin bottles to avoid physical damage to fragile protists. Nutrients were not added to incubation bottles to minimize impacts on grazing in oligotrophic waters (Lessard & Murrell 1998). Niskin bottles were also sampled (300 ml) for 16S sequence analysis of the initial (ambient) composition of the bacterial community, and each filled bottle was subsampled for flow cyto-

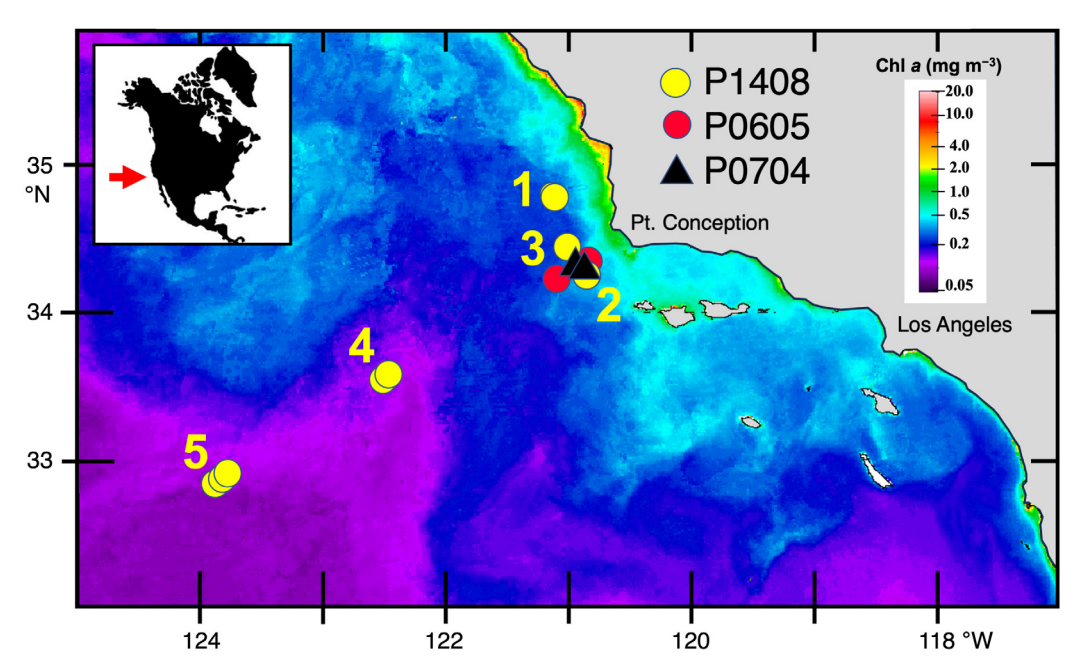


Fig. 1. Sampling and experimental locations in the California Current Ecosystem (CCE). Sites 1–5 (yellow) are for Process cruise (P1408) during anomalous warm-water, low-upwelling conditions in 2014. Red and black symbols are inshore sampling sites during normal upwelling years in 2006 (P0605) and 2007 (P0704). Chl α is merged ocean color product from MERIS, MODIS-Aqua and MODIS-Terra data for August 2014 (courtesy M. Kahru)

metry (FCM) analysis (1-2 ml) for initial HBact concentrations. The bottles were then placed in coarse net bags, attached to the line below the drifter float and incubated *in situ* for 24 h at the depth of collection. Upon array recovery, each bottle was subsampled for final HBact cell abundances by FCM and community composition by 16S sequence analysis.

During most multiday drifter experiments, we also prepared one traditional multi-treatment dilution experiment (Landry & Hassett 1982) to assess linearity. This was done with mixed-layer water (typically 10 m) collected from an evening hydrocast in the same water parcel sampled for the 2-treatment incubations. For P0605, however, the linearity experiment comes from water collected directly downstream of the upwelling center because the original experiment was not subsampled for flow cytometry. The general setup for these experiments was similar to the early morning 2-treatment experiments, but details differed in several respects: (1) treatments were replicated; (2) the main dilution series of $\sim 20\%$, 40%, 60%, 80% and 100% natural seawater was spiked with a nutrient mixture (5 µM nitrate, 0.5 M phosphate); (3) replicated control treatments were used to assess nutrient stimulation effects on growth rate estimates (Landry et al. 1998); (4) the experiments were subsampled for HBact abundance by FCM but not for sequence analyses; and (5) the bottles were incubated for 24 h in a shipboard incubator (cooled by surface seawater, 30% incident light), rather than *in situ* on the drifter array.

2.2. Bacteria cell abundances and community composition

Samples for FCM enumeration of HBact abundances were preserved with 0.5% paraformaldehyde (final concentration), flash frozen in liquid nitrogen and stored at $-80\,^{\circ}\text{C}$. Thawed samples were stained with Hoechst 33342 (1 μg ml $^{-1}$, final concentration) immediately prior to analysis (Monger & Landry 1993) on a Beckman-Coulter Altra flow cytometer equipped with a Harvard Apparatus syringe pump to quantify volume sampled, and 2 argon ion lasers tuned to UV (200 mW) and 488 nm (1 W) excitation. Listmode files were analyzed with FlowJo software to distinguish HBact from photosynthetic microbes based on presence of DNA (all cells), absence of photosynthetic pigments and forward angle light scatter (relative size).

Samples (300 ml) for prokaryote sequence analysis were collected from the CTD Niskin bottles for initial measurements and from each dilution bottle at the end of the 24-h incubations. The samples were filtered onto 0.2- μm Supor filters, flash frozen in liquid nitrogen and stored at -80° C until analysis. DNA was

extracted using the NucleoMag 96 Plant kit. Amplicon libraries targeting the V4-V5 region of the 16 S rRNA gene (515F GTG YCA GCM GCC GCG GTA and 926 R CCG YCA ATT YMT TTR AGT TT) (Parada et al. 2016) were generated as described at https://www.protocols. io/view/amplicon-library-preparationbmuck6sw. Briefly, DNA was amplified via a 1-step PCR using the TruFi DNA Polymerase PCR kit (Azura). Each reaction was performed with an initial denaturing step at 95°C for 1 min followed by 30 cycles of 95°C for 15 s, 56°C for 15 s and 72°C for 30 s. A volume of 2.5 µl of each PCR reaction was run on a 1.8% agarose gel to confirm amplification. PCR products were purified using Beckman-Coulter AMPure XP beads following the standard 1× PCR clean-up protocol. PCR quantification was performed in duplicate using the Invitrogen Quant-iT PicoGreen dsDNA Assay kit. Samples were then pooled in equal proportions followed by an additional 0.8× AMPure XP bead purification. The pool was evaluated on an Agilent 2200 TapeStation, quantified with Qubit HS dsDNA and sequenced with Illumina on the MiSeq platform with 600 cycles producing 2×300 bp paired-end reads.

Illumina sequencing reads were processed to remove primer and adapter fragments, and fastq files were input into the rRNA pipeline written by J. P. Mc-Crow (https://github.com/allenlab/rRNA_pipeline). Paired-end reads were combined using pear (Zhang et al. 2014) with a -t parameter for minimum trim length of 50 bp. Chimeric sequences were identified and removed using usearch (Edgar 2010), with the -strand plus parameter set. Reads were then quality trimmed to Q25 average quality across a window of 2 bases using the fastq filter.py script. Amplicons were clustered into operational taxonomic units (OTUs) using swarm (Mahé et al. 2014) with default parameters, and further filtered to require at least 3 reads across at least 2 samples. Taxonomic best hits were assigned by glsearch36 (Pearson 2016), with default parameters. The SILVA database was used as a reference for 16S rRNA sequences (Quast et al. 2012, version 111), with OTUs classified as potential plastid sequences separated and reclassified with PhtyoRef (Decelle et al. 2015). Non-plastid eukaryotic sequences were removed from the analysis. The samples analyzed yielded a total of 3970 16S OTUs, most relatively rare, and averaged (\pm SEM) 17 200 \pm 1000 HBact reads per sample (excluding cyanobacteria).

Cell abundance estimates of select (dominant) bacterial taxa were determined, assuming one read per cell, from total FCM counts of HBact in a given sample (CTD or experimental bottle) and the correspond-

ing relative taxon contributions to total 16S reads in that sample. Abundance estimates from CTD sampling (experimental initials) are presented as ambient cell concentrations and are also the basis for computing net rates of change of the ambient community from samples collected on different days following the drifter array. As described further below, we used taxon-specific abundance estimates from initial and final samples of dilution experiments as the data for estimating cell growth rates of dominant HBact groups. Implications of the one read per cell assumption as a potential rate bias factor are considered in the Discussion section.

2.3. Growth rate determinations

For dilution experiments, we computed net growth rates from initial and final cell abundances in undiluted (k) and diluted (k_d) treatments as:

$$k = 1/t \times \ln(P_t/P_0) \tag{1}$$

and

$$k_{\rm d} = 1/t \times \ln(P_{\rm t,d}/[DP_0])$$
 (2)

where t is experiment duration (1 d), $P_{\rm t}$ and $P_{\rm t,d}$ are final bacteria cells ml⁻¹ in undiluted (control) and diluted treatments, respectively, and $P_{\rm 0}$ is initial abundance in the undiluted treatment. HBact cell counts from FCM analyses of the initial diluted treatments ($P_{\rm 0,d}$) were used to determine mean dilution factors $D_{\rm 0}$ from the ratios of $P_{\rm 0,d}$ to $P_{\rm 0}$. We applied the average $D_{\rm 0}$ to all experiments that used the same volumetric ratios of filtered and natural seawater to avoid transferring random subsampling errors to the rate calculations that come from incomplete mixing of natural and filtered waters during the filling and subsampling process.

For 2-treatment dilution experiments, we computed instantaneous estimates of cell division rates (hereafter = growth rates, μ , d^{-1}) from the net growth estimates for the 2 experimental bottles as: $\mu = k + ([k_d - k]/[1 - D])$ (Landry et al. 2008, 2011). For the full dilution experiments incubated shipboard, growth rates are determined as the y-intercept of the regression relationships between treatment net growth rates (k, k_d) and treatment dilution factors for the dilution series with added nutrients (Landry & Hassett 1982). Since these experiments are presented mainly to illustrate general results from that approach, we show but do not use results from the no-nutrient control bottles to refine the growth rate estimates (Landry et al. 1998).

2.4. Environmental data and ancillary measurements

Temperature, nutrient, chlorophyll a (chl a) and productivity data are from the CCE-LTER data website (https://oceaninformatics.ucsd.edu/datazoo/catalogs/ ccelter/datasets) for the same hydrocasts and depths as the dilution experiments. Temperature was measured by CTD sensors at the depth of water collection. Nutrient samples were filtered through an in-line 0.1- μ m Suporcap capsule, frozen at -20°C, and subsequently analyzed in the laboratory against prepared standards by continuous-flow autoanalyzer or flow injection techniques. Chl a samples (250 ml) were filtered onto GF/F filters, extracted with 90% acetone at -4° C for 24 h, and run shipboard with a calibrated Turner Designs model 10 fluorometer. Primary production measurements were done in triplicate 250 ml bottles using the ¹⁴C method, using water from the same hydrocasts, and incubated in situ in the same net bags and depths as dilution experiments.

2.5. Statistical tests

All statistical tests were conducted with the Microsoft Excel Data Analysis package (version 16.79.2, 2023). Mean comparisons are 2-sided *t*-tests for un-

equal variance, $\alpha = 0.05$. Regression slope significance is evaluated for 95% confidence limits.

3. RESULTS

3.1. Environmental conditions

Table 1 presents environmental conditions for the samples and experiments analyzed, with experiments 14.1-14.3c corresponding to P1408 inshore sites 1-3 (hereafter, inshore) in Fig. 1. Experiments 14.4a-14.5 d correspond to P1408 offshore sites 4 and 5 (hereafter, offshore), and 06.1a-07.2b are the upwelling sites for cruises P0605 and P0704 (hereafter, upwelling). With the exception of 14.3c, which hit the upper thermocline at 35 m at site 3, samples from the upper 25 m (to 40 m at offshore site 5) represent conditions in the mixed upper euphotic zones of the experimental stations. We use integrated primary production to 30 m depth (IPP30) as an index of the productivity relevant to bacteria residing in the mixed upper ocean at each station.

The experiments divide naturally into 3 groups based on nitrate, chl a and IPP30 (Table 1). Temperature also varies but has less diagnostic value, as the P1408 cruise was during an unprecedented heatwave in which upper 50-m seawater temperatures reached $4-5^{\circ}\mathrm{C}$ above seasonal averages (Zaba & Rudnick

Table 1. Locations, dates, depths and environmental variables for experimental samples analyzed for community composition and growth rates (*community composition only). Chl a: chlorophyll a; HBact: heterotrophic bacteria flow cytometry cell counts; IPP30: integrated primary production to 30 m depth

Cruise	Expt ID	Date (mm/dd/yyyy)		Longitude (°W)	Depth (m)	Temperature (°C)	NO ₃ (μΜ)	Chl <i>a</i> (mg m ⁻³)	HBact $(10^6 \mathrm{cells} \mathrm{ml}^{-1})$	IPP30 (mg C m ⁻² d ⁻¹)
P1408	14.1	08/13/2014	34.81	121.22	12	16.49	0.02	0.661	1.09	411
P1408	14.2a	08/17/2014	34.27	120.82	12	16.74	0.05	0.694	0.92	303
P1408	14.2b	08/19/2014	34.12	120.92	12	16.90	0.05	0.841	1.79	297
P1408	14.3a	08/22/2014	34.39	121.39	12	18.32	0.04	0.202	1.66	218
P1408	14.3b*	08/24/2014	34.43	121.15	12	18.11	0.02	0.239	1.48	234
P1408	14.3c	08/24/2014	34.43	121.15	35	13.02	5.13	0.713	0.88	234
P1408	14.4a	08/26/2014	33.52	122.56	12	18.98	0.04	0.111	1.17	68
P1408	14.4b	08/27/2014	33.54	122.51	12	19.23	0.05	0.097	1.02	70
P1408	14.5a	08/30/2014	32.88	123.89	20	19.23	0.04	0.096	0.73	64
P1408	14.5b	08/31/2014	32.84	123.87	20	19.63	0.01	0.090	0.63	59
P1408	14.5c	09/01/2014	32.81	123.87	20	19.80	0.04	0.082	0.62	64
P1408	14.5d	09/01/2014	32.81	123.87	40	17.95	0.03	0.121	0.89	64
P0605	06.1a	05/11/2006	34.33	120.80	12	11.32	13.6	3.01	1.06	2617
P0605	06.1b	05/11/2006	34.33	120.80	25	11.24	13.7	3.07	0.99	2617
P0605	06.2a	05/14/2006	34.26	120.80	12	12.30	10.8	6.40	2.49	2594
P0605	06.2b	05/14/2006	34.26	120.80	25	12.29	16.7	6.38	2.46	2594
P0704	07.1a*	04/04/2007	34.26	120.84	12	12.33	9.00	2.26	1.44	2408
P0704	07.1b*	04/04/2007	34.26	120.84	25	12.15	9.03	2.20	3.04	2408
P0704	07.2a*	04/05/2007	34.28	120.91	12	12.09	8.17	1.58	1.09	1016
P0704	07.2b	04/05/2007	34.28	120.91	25	12.03	9.00	1.47	1.11	1016

2016), while P0605 and P0704 samples were taken 4-5 mo earlier in the annual cycle as well as selected for high upwelling, hence mixing of cool, deep water into the surface layer. The offshore experiments are representative of intense stratification and oligotrophy, with uniformly low nitrate, chl a and productivity $(0.04 \pm 0.002 \,\mu\text{M}, 0.10 \pm 0.002 \,\text{mg chl} \,a\,\text{m}^{-3} \,\text{and} \,65 \pm$ $1 \text{ mg C m}^{-3} \text{ d}^{-1}$, respectively). Inshore P1408 experiments have similarly low nitrate (excluding 14.3c) but 4-5 fold higher chl a and IPP30 (0.56 \pm 0.04 mg chl a m^{-3} and 283 \pm 12 mg C m^{-3} d⁻¹, respectively). Upwelling experiments from the earlier cruises represent an even more substantial step up in environmental richness, with mean nitrate, chl α and production values of 11.2 \pm 0.4 μ M, 1.7 \pm 0.1 mg chl a m⁻³ and 2160 \pm 89 mg C m⁻³ d⁻¹, respectively. Overall, the sample groups differ by 33-fold in both phototrophic biomass and production, but only by a factor of 2 for HBact cell abundances $(0.84 \pm 0.04 \text{ versus } 1.71 \pm 0.10 \times 10^6 \text{ cells})$ ml^{-1} for offshore and upwelling, respectively).

3.2. Bacteria abundances and community composition

Fig. 2 presents mean estimates of bacterial cell abundances and percent contributions to the total HBact community for dominant taxa at the offshore, inshore and upwelling sites. The top panels (Fig. 2a,b) are for the major groups of Proteobacteria (alpha, gamma and beta), Bacteriodes (Flavobacteria are 96.4% of Bacteriodes in our samples, and all rate determinations for Flavobacteria give the same results for Bacteriodes) and Verrucomicrobia, which together account for 95.6% of all 16S sequence reads. The bottom panels (Fig. 2c,d) are for dominant (sub)taxa within the major groups, which account for 62-73% of all sequence reads. SAR11 (Pelagibacter), Rhodobacteraceae and SAR116 (Rickettsiales) are the main subgroups of Alphaproteobacteria, and SAR86 (Oceanospirillales) is the dominant Gammaproteobacteria. Bacteriodes/

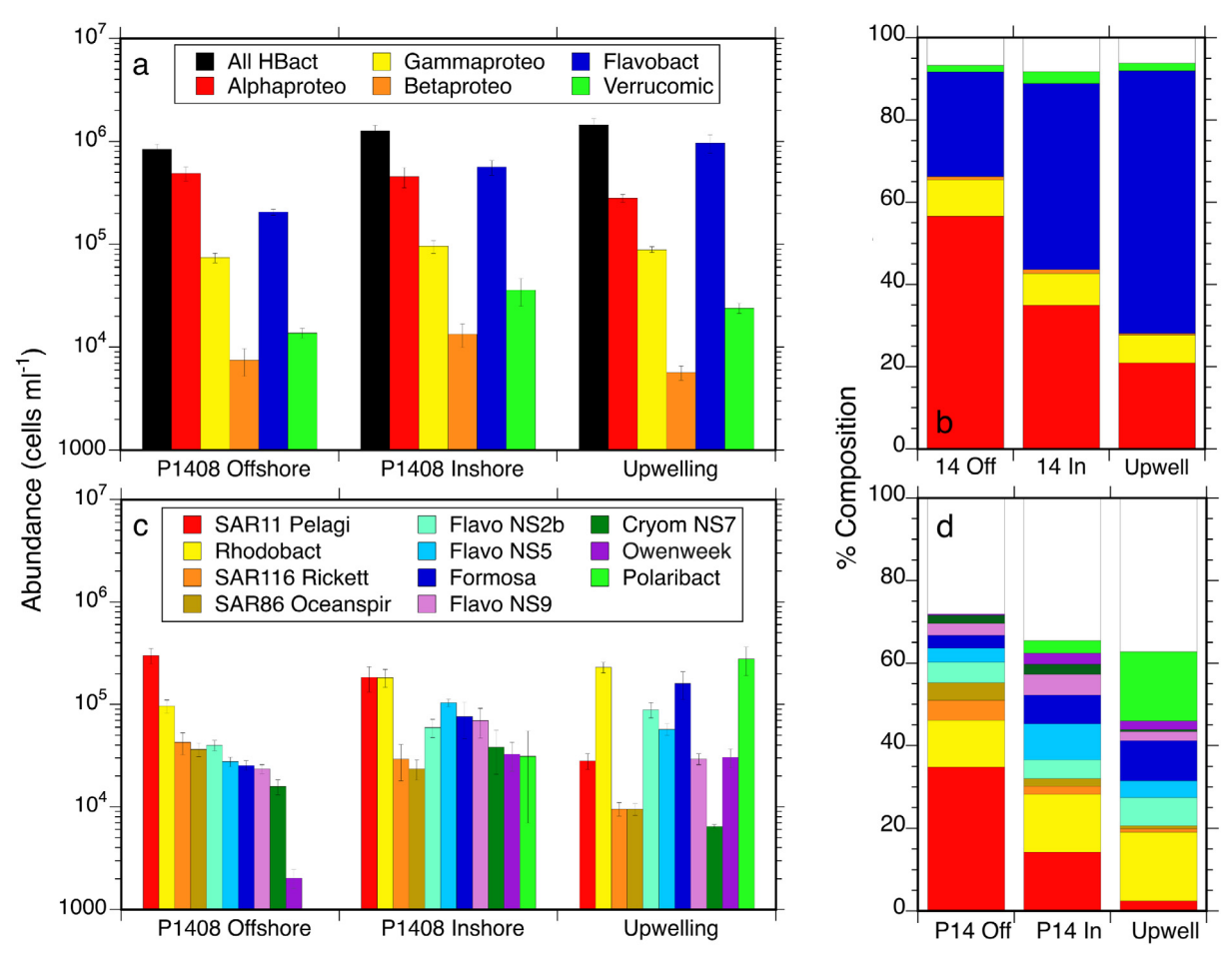


Fig. 2. Mean abundances and percent contributions of heterotrophic bacteria (HBact) at offshore and inshore locations sampled in 2014 and at inshore upwelling locations sampled in 2006 and 2007. (a,b) Total HBact and major groups. (c,d) Lower-level taxa comprising the largest portion of total HBact. Uncertainties are SEM values. Full names of bacteria are given in Table 2

Flavobacteria are represented by 5 subgroups of Flavobacteriaceae (*Formosa*, *Polaribacter* and marine groups NS5, NS2b and NS9) and 2 subgroups of Cryomorphaceae (marine group NS7 and *Owenweeksia*).

Most taxa differed modestly in mean cell abundances or percent composition over the range of environmental conditions examined (Fig. 2a,b). Among major taxa exceptions, Alphaproteobacteria dominated numerically and compositionally (0.49 \pm 0.08 \times 10⁶ cells ml $^{-1}$ and 56.5 \pm 3.2%, respectively) at oligotrophic offshore sites, but declined to 0.28 \pm 0.02 \times 10⁶ cells ml $^{-1}$ and 20.9 \pm 2.0% in rich upwelling waters. Conversely, Flavobacteria increased from 0.21 \pm 0.01 to 0.96 \pm 0.20 \times 10⁶ cells ml $^{-1}$ (25.4 \pm 2.4 to 63.8 \pm 3.2%, respectively) from offshore to upwelling sites. Inshore sites had intermediate abundances and percent contributions of Alphaproteobacteria and Flavobacteria.

Among the subgroups examined, SAR11 and Polaribacter varied the most with system richness (Fig. 2c,d). SAR11 declined by an order of magnitude, from 0.30 ± 0.05 to $0.028 \pm 0.005 \times 10^{6}$ cells ml⁻¹ (34.8 ± 2.8 to $2.4 \pm 0.5\%$ contribution), between offshore and upwelling samples. Polaribacter increased with richness, from negligible concentration (<100 cells ml⁻¹) for offshore to 0.28 \pm 0.09 \times 10⁶ cells ml⁻¹ (16.8 \pm 2.4%) in the upwelling samples. Flavobacteria taxa Formosa, NS2b and Owenweeksia followed that major group's trend of increasing with richness. SAR116 and SAR86 followed the general Proteobacteria trend of decreasing with increasing system richness, but Rhodobacteria ran counter to the trend by increasing in abundance and relative importance (from 11.3 ± 1.0 to $16.7 \pm 1.4\%$). Overall, dominance structure of the HBact community varied from predominance of SAR11 in the most oligotrophic waters to co-dominance of Polaribacter, Rhodobacteria and Formosa in rich upwelling conditions, with codominance of SAR11 and Rhodobacteria (both Alphaproteobacteria) in the P1408 upwelling-suppressed inshore waters of moderate productivity.

3.3. Bacteria growth rates

The full dilution experiments incubated shipboard generally confirm the assumed linearity between net growth rates and dilution factor on average (Fig. 3a—d), though treatments showed considerable variability in some cases (Fig. 3b,f). Most net growth rates were positive, but Fig. 3a (P1408 site 1 in Fig. 1; 14.1 in Table 1) is an example of HBact cell decline in all dilu-

tion treatments that is not grazer driven and is more likely due to viral lysis.

For the subset of 2-treatment dilution experiments analyzed, growth rates of the HBact community increased 2-fold on average, from 0.33 ± 0.03 to 0.62 \pm 0.05 d⁻¹, between offshore and upwelling results (Fig. 4a). Because uncertainties are large, growth rates of most major taxonomic groups did not differ statistically from the community averages. Alphaproteobacteria stood out, however, in having significantly higher than mean rates at the environmental extremes, varying from 0.50 ± 0.07 (p = 0.008, t-test unequal variance) for offshore to $1.17 \pm 0.14 \,\mathrm{d}^{-1}$ (p = 0.012) for upwelling experiments. In contrast, growth rates of Bacteriodes/Flavobacteria were lower than HBact averages for these same conditions (0.00 ± 0.08) and $0.30 \pm 0.23 \,\mathrm{d}^{-1}$, respectively), but the difference was only significant for offshore results (p = 0.02).

Similarly, among subtaxa that comprise the major groups, only a few differed significantly from community average growth rates, and these were only for experiments at the environmental extremes, not inshore (Fig. 5a). Growth rates of SAR11 were higher than the HBact mean for both offshore $(0.51 \pm 0.06 \,\mathrm{d}^{-1})$, p = 0.03) and upwelling conditions (1.53 ± 0.27 d⁻¹, p = 0.03). Growth rates of the Alphaproteobacteria codominant Rhodobacteria were lower than the HBact average under offshore oligotrophic conditions (-0.23 \pm 0.09 d⁻¹, p = 0.001) but higher than average in upwelling experiments (1.11 \pm 0.15 d⁻¹, p = 0.036). Among the 3 Flavobacteria taxa (Formosa, NS5, NS9) with growth rates that appeared to differ from the HBact mean, only the lower-than-average and negative estimates for NS5 were significant ($-0.16 \pm 0.13 \,\mathrm{d}^{-1}$, p = 0.009 for offshore; $0.03 \pm 0.13 d^{-1}$, p = 0.005 for upwelling).

Net growth rates for the HBact community trended upward with increasing richness, from slightly negative $(-0.13 \pm 0.05 \,\mathrm{d}^{-1}; \,\mathrm{grazing} > \mathrm{cell} \,\mathrm{growth})$ for offshore to close to balanced (0.07 \pm 0.06 d⁻¹; grazing \approx growth) for inshore, and positive (0.17 \pm 0.04 d⁻¹; grazing < growth) for upwelling experiments (Fig. 4b). For P1408 offshore and inshore experiments, net growth of individual major groups and subtaxa generally conformed, within experimental variability, to the HBact averages (Figs. 4b & 5b). The only significant difference was the lower-than-average net growth rate of Rhodobacteria in the offshore experiments (p = 0.0008; Fig. 5b). For experiments conducted during upwelling conditions, net growth rates suggest that different populations were increasing or decreasing substantially. We examine those closer in the subsection below.

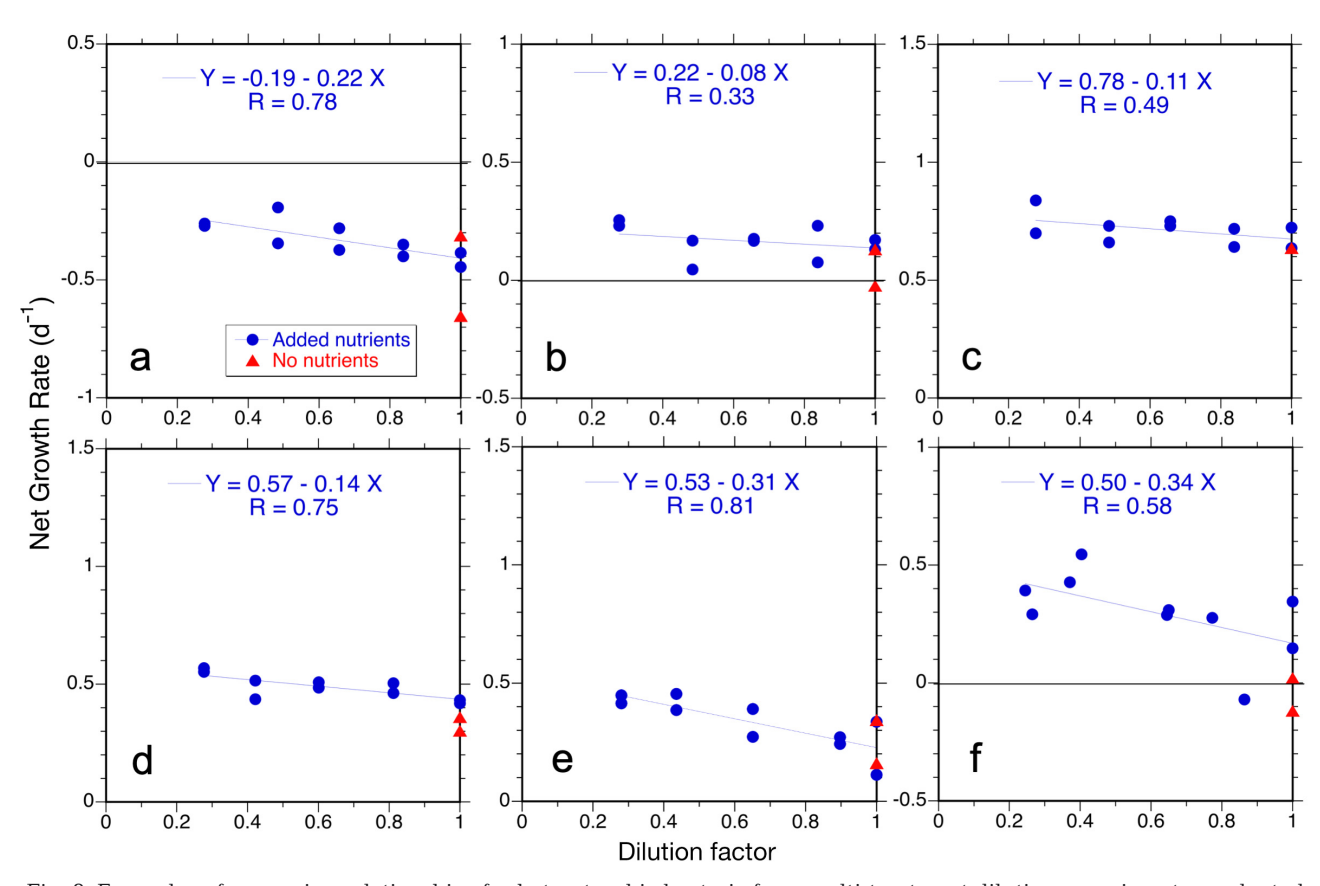


Fig. 3. Examples of regression relationships for heterotrophic bacteria from multi-treatment dilution experiments conducted during CCE Process cruises. (a—d) Samples from P1408 at locations 1—4 (see Fig. 1), respectively. (e,f) Samples from P0605 and P0704 upwelling experiments, respectively. Blue symbols are for treatments with added nutrients. Red symbols are for control incubations without added nutrients

3.4. Net growth rates during an upwelling bloom

The inclusion of one experiment from P0704 (07.2b in Table 1) during a bloom decline partially offsets the upwelling rate trends from 4 P0605 experiments that were performed during active bloom growth. Having been conducted at 2 depths 3 d apart following a satellite-tracked drifter, the P0605 environmental sampling and experiments also allow, by themselves, an unambiguous comparison between net population growth rates in the ambient water over the time period of sampling and the net rates determined in bottle experiments incubated at the same depths on the drifter array (Table 2). In the P0605 samples, total HBact cell abundance more than doubled in the water column over 3 d, giving a mean net grow rate of $0.29 \pm$ 0.01 d⁻¹. Flavobacteria dominated numerically and increased by > 3-fold (0.43 \pm 0.03 d⁻¹), led mainly by increasing Formosa (0.51 \pm 0.05 d⁻¹) and Polaribacter $(0.46 \pm 0.02 \,\mathrm{d}^{-1})$. Alphaproteobacteria, the secondary major group, exhibited lower and more variable net growth $(0.10 \pm 0.09 \,\mathrm{d}^{-1})$, divided between increasing

Rhodobacteria (0.16 \pm 0.10 d⁻¹) and rapidly decreasing abundances of SAR11 (-0.44 ± 0.03 d⁻¹) and SAR116 (-0.34 ± 0.03 d⁻¹).

Net growth rates in the incubated experimental bottles showed the same general trends and relative rates as observed in the water-column samples, especially for populations that were dominant or exhibited high positive or negative rates of change (Fig. 6). Populations with low cell abundance or little net change, such as NS9, NS7 and Betaproteobacteria, were captured less well in experimental results, but the relationship between ambient observed and experimentally determined net growth rates was highly significant overall (p = 0.0004).

4. DISCUSSION

The major objective of the present study was to evaluate a dilution-based approach that combines FCM measurements of total HBact with 16S sequence analysis of relative abundances to estimate population-

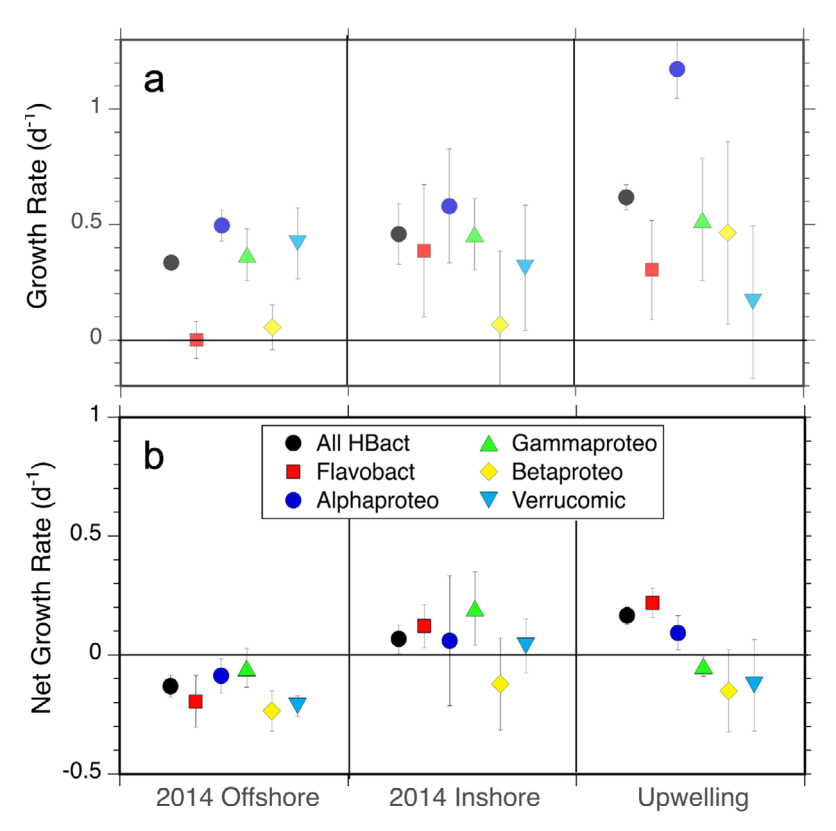


Fig. 4. Growth rates of major groups of heterotrophic bacteria (corresponding to Fig. 2a,b) at offshore and inshore locations in 2014 and inshore upwelling locations in 2006 and 2007. (a) Estimates of instantaneous growth rates. (b) Estimates of net growth rates after grazing mortality. Uncertainties are SEM values

specific rates of bacterial cell growth. Below, we first consider various aspects of that approach as they relate to general assumptions of dilution experiments, specific additional concerns for applications to HBact, the magnitude of uncertainties in rate estimates, sequence analysis issues that might bias rate results, and suggestions for improvement. We then interpret net growth and growth rate results.

4.1. General methodological considerations

The basic dilution approach assumes a linear increase of net growth rate with dilution factor and similar growth conditions in all treatments (Landry & Hassett 1982, Landry 1993). In general, results of the multi-treatment dilution support the linearity assumption for the range of environmental circumstances that we examined. Even where nonlinearities can be reasonably argued (e.g. Fig. 3b,f), 2 treatments of ~30% and 100% will typically produce rate results similar to the larger experiments. While nutrients are not expected to influence growth rates of HBact directly, their addition could indirectly affect HBact

by stimulating co-occurring phytoplankton. In this regard, most of the full dilution results show net growth estimates for no-nutrient treatments that are slightly lower on average ($\sim 0.095 \pm 0.041 \, d^{-1}$) than nutrient-added bottles. Since even a small offset can be meaningful relative to the low growth rates of HBact, this interpretative complication is avoided by not adding nutrients.

Because 0.1- or 0.2-µm filters used for preparing dilution treatments are too coarse to remove viruses as a mortality agent, the standard dilution approach does not account for the component of bacterial growth that is lost to viral lysis. Nonetheless, viral impacts can be measured relative to standard dilution growth-grazing results using a modified approach with 30-kDa filtered water (Baudoux et al. 2008, Pasulka et al. 2015), and this could be adapted for use with FCM-normalized rRNA gene sequences, similar to the present study. Additionally, the ratio of extracellular ribosomal RNA (rRNA_{ext}) produced by viral lysis to cellular rRNA of the bacterial community has been advanced as a potential index of taxon-specific viral

mortality in the natural environment (Zhong et al. 2023), and could potentially be used in combination with modified dilution assays to better understand the relative impacts of lysis and grazing on bacterial community dynamics.

In applying the dilution approach specifically to HBact, the additional concerns are possible alteration of community composition by bottle containment (Massana et al. 2001, Gattuso et al. 2002, Hammes et al. 2010) and potential growth stimulation from DOM released during the seawater filtration process for preparing dilution treatments (Fuhrman & Bell 1985, Pree et al. 2016). Regarding the first concern, we found little evidence for dramatic shifts in HBact community composition for the suite of taxa examined in our incubations. To the contrary, and highlighting an advantage of Lagrangian-designed studies, the trajectories of microbial community change in experimental bottles paralleled and generally explained those that we observed in the ambient environment (Fig. 6 and discussed further below).

Regarding the second concern, some DOM release into seawater filtrate for our experiments would seem likely, but whether this leads to excessive estimates of

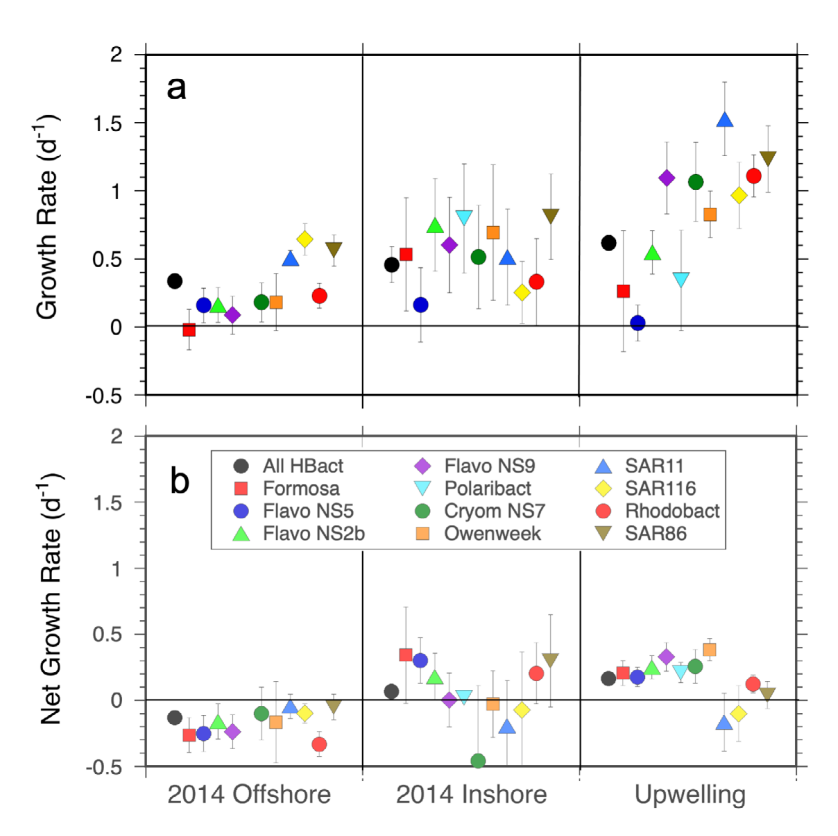


Fig. 5. Growth rates of abundant subgroups of heterotrophic bacteria (corresponding to Fig. 2c,d) at offshore and inshore locations in 2014 and inshore upwelling locations in 2006 and 2007. (a) Estimates of instantaneous growth rates. (b) Estimates of net growth rates after grazing mortality. Uncertainties are SEM values

HBact growth is questionable. For example, our growth rate estimates for CCE offshore waters $(0.29 \pm 0.03 \text{ d}^{-1})$ are almost 3-fold lower, and even upwelling rates $(0.58 \pm 0.06 \,\mathrm{d}^{-1})$ are 30% lower, compared to recent growth rate estimates $(0.80-0.85 d^{-1})$ from oligotrophic subtropical waters based on turnover of bacterial phospholipids and bacteriochlorophyll a (Popendorf et al. 2020). The general magnitude of upwelling rates are also supported by water-column observations of abundance increases, net of mortality losses, that are almost as high for some populations $(0.4-0.5 d^{-1}; Table 2)$ as the community growth estimates from bottle incubations inclusive of grazing. Thus, sustained rates of the magnitude measured in bottles are clearly observable in the natural environment. Previous studies also suggest that filtration enrichment of DOM should be greatest for richer coastal and bloom waters with high plankton biomass (Fuhrman & Bell 1985, Pree et al. 2016). However, we found no systematic bias between rich and poor waters when comparing dilution-based estimates of

Table 2. Population cell abundance and growth rates determined from Lagrangian resampling during upwelling conditions on P0605. D1 and D4 are Day 1 and Day 4 sampling following the satellite-tracked drifter. Mean (\pm SEM uncertainties) of net growth rates (d⁻¹) in the ambient water column are computed from the net D1 and D4 changes of population abundance at 2 depths, 12 and 25 m. Experiment rates (d⁻¹) are determined from net growth in dilution experiments incubated *in situ* at 12 and 25 m on D1 and D4

Taxon -	F	opulation abund	$$ Net growth rate (d^{-1}) $$			
	D1, 12 m	D1, 25 m	D4, 12 m	D4, 25 m	Ambient	Experiment
All HBact	1 060 000	990 000	2 490 000	2 460 000	0.29 ± 0.01	0.20 ± 0.02
Flavobacteria	493 000	570 600	1894000	1800000	0.42 ± 0.03	0.28 ± 0.02
Alphaproteobacteria	352 000	215 000	362 000	373 000	0.10 ± 0.09	0.03 ± 0.05
Gammaproteobacteria	109 000	89 700	109 000	103 000	0.02 ± 0.02	-0.06 ± 0.05
Betaproteobacteria	5980	8630	5140	10 300	0.00 ± 0.06	-0.28 ± 0.15
Verrucomicrobia	14800	12700	18 390	25 000	0.15 ± 0.08	0.00 ± 0.18
Formosa	72 700	92 100	390600	272 000	0.51 ± 0.05	0.29 ± 0.04
Flavo NS5	27 700	42 100	89 900	85 000	0.31 ± 0.08	0.21 ± 0.09
Flavo NS2b	17 300	29 100	90 200	94 100	0.47 ± 0.08	0.30 ± 0.09
Flavo NS9	41 000	33 300	26 900	46 800	-0.01 ± 0.13	0.31 ± 0.14
Polaribacter	172 000	167 000	716 000	625 000	0.46 ± 0.02	0.28 ± 0.03
Cryom NS7	7350	6930	5140	5650	-0.09 ± 0.03	0.23 ± 0.16
Owenweeksia	27 400	25 100	46 900	68 200	0.26 ± 0.08	0.33 ± 0.09
SAR11 (Pelagibacter)	40 900	24600	11800	6010	-0.44 ± 0.03	-0.30 ± 0.22
SAR116 (Rickettsiales)	17 900	10 590	6040	4210	-0.34 ± 0.03	-0.24 ± 0.20
Rhodobacteria	274000	160 000	331 000	350 000	0.16 ± 0.10	0.08 ± 0.06
SAR86 (Oceanospirillales)	16 400	11 200	10 900	9970	-0.09 ± 0.05	0.04 ± 0.13

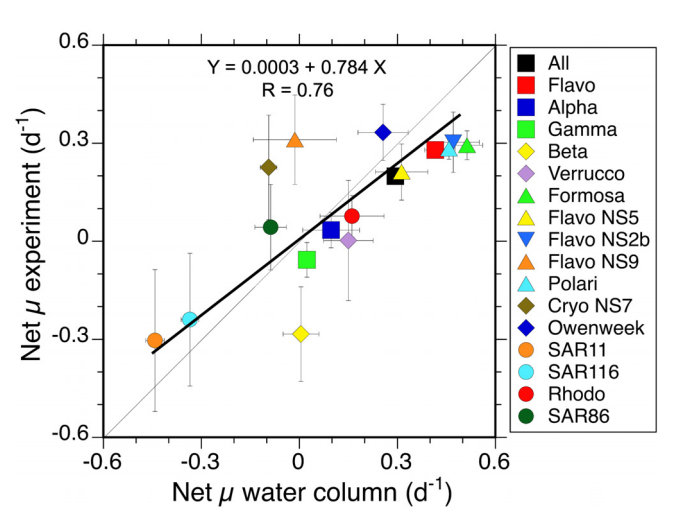


Fig. 6. Comparison of net growth rate (net μ) estimates of heterotrophic bacteria from dilution incubations (y-axis) to net observed growth rates in the ambient water column (x-axis) following a drogued drifter for 5 d during an upwelling bloom in 2006. Regression relationship is Model 2 reduced major axis. Uncertainties are SEM values

bacterial carbon production (BCP) to standard ³Hleucine rates for 3 CCE Process cruises, including P1408 (Landry et al. 2023). Further, for cell carbon conversions informed by size variability from flow cytometry, the 2 BCP estimates displayed a 1:1 regression relationship (Landry et al. 2023), which would leave little room for substantial systematic overestimation of the dilution growth rates. Fuhrman & Bell (1985) did note, however, that coarser filters (GF/F and 1-µm membrane) of the types used to separate bacteria from grazers in dilution culture and growth-rate manipulation studies (e.g. Ferrera et al. 2011, Alonso-Sáez et al. 2010) resulted in the highest release of dissolved free amino acids, which we associate below with the tendency of such manipulations to yield much higher HBact growth rate estimates than the present study.

4.2. Uncertainties in rate determinations

As would be expected with an added layer of analytical error, apportioning FCM estimates of total HBact abundance to relative sequence reads significantly amplifies the resulting uncertainties in sequence-based growth rate estimates compared to the relatively modest values from FCM (Figs. 4 & 5). To understand better how uncertainty might be predicted or reduced in future studies, we examine the error relationships more closely in Fig. 7 for populations of varying abundance. Overall, relative uncertainty (FCM = 1.0) increases substantially for populations of lower abundance and increasing rarity.

However, among individual groups, only the relationship for offshore experiments is significant (p = 10^{-6} , blue line in Fig. 7). For the upwelling experiments, several dominant populations with high abundances show larger relative uncertainties than expected from the offshore relationship (Flavobacteria = 3.9; Formosa = 7.7; Polaribacter = 6.4). For inshore experiments, relative uncertainties fall below the line for some rarer taxa (Gammaproteobacteria = 1.2; NS4 = 1.4; SAR116 = 1.8). The reasons for these departures are unclear, but might relate to differences in coherence of experiments within their groupings. Offshore experiments were all performed under relatively constant oligotrophic environmental conditions. In contrast, both inshore (Sites 1-3) and upwelling (P0605 and P0704 cruises) groupings are mixtures of experiments with different station origins and dynamics.

In general, assuming total HBact abundances on the order of $10^6 \, \mathrm{ml^{-1}}$, semi-dominant populations comprising 10% or more of total cells (i.e. $> 10^5 \, \mathrm{cells} \, \mathrm{ml^{-1}}$) have growth uncertainties 2–3 times greater than FCM values, therefore requiring 4 to 9 times more experiments to match the same confidence levels as the FCM results. For populations comprising ~1% (i.e. $10^4 \, \mathrm{cells} \, \mathrm{ml^{-1}}$) of community abundance, expected relative uncertainty is about 4 times greater than

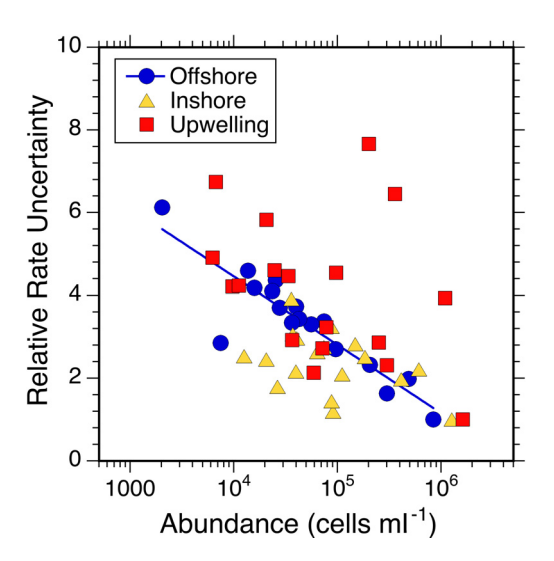


Fig. 7. Relative uncertainties of bacterial growth rate estimates for sequence-defined populations of varying abundances relative to growth rate uncertainties from flow cytometry. Uncertainties for flow cytometry rate estimates for the total HBact community are plotted at 1.0 (lower right) for 3 experimental groups: P1408 offshore, P1408 inshore and P0605–P0704 upwelling. The regression relationship for offshore experiments is $y=11.06-1.65\log x$, R=0.90, $p=10^{-6}$. Individual regressions for inshore and upwelling experiments are not significant

growth rate estimates from FCM. To achieve reasonable confidence levels for growth rate estimates of all, but especially rare, populations, uncertainties arising from random analytical variability might be substantially reduced by improvements in protocols for extracting and amplifying sequences, by including analytical standards (e.g. Fecskeová et al. 2021) and by increasing the number of sequence reads per sample (well above the current average of 17 000 reads).

4.3. Potential for sequence-related bias

We made the assumption above that sequence reads directly translate to relative cell abundances in the environment mainly for the purpose of providing a numerical basis for rate calculations. Although this ignores known variability in 16S rRNA gene copy number among and within bacterial taxa, the proposed computational corrections for such variability are complex, imprecise and would make our community profiles difficult to compare to 16S results for other marine systems (Louca et al. 2018). The database for ribosomal RNA operon copy number (rrnDB; Stoddard et al. 2015) provides some insight into how community profiles might be affected by this issue, with cell abundances of taxa with low mean copy numbers (Pelagibacter/SAR11 = 1.4, Rickettsiales/ SAR116 = 1.0) being likely underestimated in Fig. 2. Conversely, we likely overestimate the cell abundances of major groups with higher mean copy numbers (Flavobacteria = 4.0, Rhodobacteriacae = 2.8, Oceanospirillale/SAR86 = 4.4), but the extent of the effect depends on whether representatives of those taxa in the natural environment have 16S copies closer to the group means or to the lower extremes (\sim 1.0) of their ranges. Regardless, copy number variability will not affect taxon-specific growth rate calculations as long as the mean number per cell remains consistent among the initial and final samples of each experiment. Rate biases may occur, however, if there are differences in taxon copy numbers between dilution treatments, especially if the differences are large and systematic. While not feasible for all taxa, it would be possible to test for copy number consistency in dilution treatments for major groups or select dominant populations where sequence frequency and FISH cell abundances (e.g. Bennke et al. 2016), both normalized to total HBact cells, can be determined and compared.

Growth rate estimates may also be affected by PCR bias, caused by differences in the amplification efficiencies of different 16S sequences in repeated cycles of the polymerase chain reaction (Suzuki & Giovan-

noni 1996, Acinas et al. 2005). While unconsidered in most studies of microbial community composition based on sequence reads, even small differences in amplification efficiencies can greatly alter initial relative sequence abundances over many cycles and lead to different relative results for the same sample run through different cycles or conditions. We did not assess PCR bias in the present study, but suggest that it be evaluated in future applications using the procedures described by Silverman et al. (2021). This process uses replicate aliquots of the community sample run through different predetermined numbers of PCR cycles as a calibration standard and corrects the reads with a log-ratio linear model.

Uncertainties relating to the ~1% of HBact cells that pass through the 0.1-µm cartridges used to prepare filtered water for diluted treatments (Landry et al. 2023) are another source of potential bias that needs to be better constrained. For cytometry estimates of HBact growth rates, we accounted for the added abundances in initial dilution samples and assumed that their growth characteristics were representative of the community as a whole. While this may be a reasonable assumption where filtrate cells comprise a relatively small portion of total HBact in the diluted treatments, ~5% in the current experiments, it would be difficult to justify at substantially higher dilution levels (e.g. for dilution treatments of 10% natural seawater, the added 90% of filtrate water would comprise almost half of all HBact cells). This would seem to preclude using treatments with very high dilution levels to increase methodological precision, as has been recommended in some studies (Gallegos 1989, Chen 2015).

The potential bias from filtrate cells would have to come from smaller cells or taxa that more easily pass the 0.1- μm filter compared to larger cells, and therefore disproportionately enrich their sequences in the diluted treatment. If uncorrected, over-represented cells will appear to grow faster in the diluted treatments, while under-represented cells in the filtrate will have lower growth rate estimates. It is not clear, however, whether cells small enough to make it into the 0.1- μm filtrate would be subsequently retained on the membrane filters used to concentrate molecular sequencing samples. If they are not, or are very sparsely retained, the filtrate composition might have little biasing impact on rate determinations.

4.4. Net growth rate interpretations

Because they derive from 24-h *in situ* incubations of whole seawater without any dilution manipulation,

net growth rates are the most robust of our sequencebased results. We consider these rates to reflect fairly accurately the balances or imbalances of growth and loss processes in the natural environment, but they also need to be understood as small samplings of larger data sets. The 4 P0605 experiments in Table 2, for instance, show good correspondence between net rates of the HBact community in experimental bottles and in the ambient environment (0.20 \pm 0.02 versus $0.29 \pm 0.01 \, d^{-1}$, respectively; Table 2). However, among the total 24 incubations conducted over 4 d in the upper 30 m from which those 4 experiments were subsampled, the agreement is even closer, with bottle results slightly higher but not significantly different from ambient rates (0.23 \pm 0.02 versus 0.20 \pm 0.04 d⁻¹, respectively; p = 0.45). Similar agreement for HBact net growth rates is observed for 47 experiments at P1408 inshore sites 1-3 (experiment = $-0.01 \pm$ 0.04 d^{-1} ; ambient = $-0.04 \pm 0.04 \text{ d}^{-1}$; p = 0.54) and for 20 upper euphotic-zone experiments at P1408 offshore sites 4 and 5 (experiment = $-0.06 \pm 0.02 \,\mathrm{d}^{-1}$; ambient = $-0.001 \pm 0.02 \,d^{-1}$; p = 0.07), for which the latter are also substantially less negative on average than the few experiments selected for sequence analysis (Figs. 4 & 5).

Overall, P0605 upwelling results capture the system during a sustained period of high productivity and net community change, while P1408 inshore and offshore results reflect dynamic steady-state conditions, but with considerable day-to-day variability in both water-column and experimental rates. Quasi steady-state dynamics are expected for the CCE offshore region, but they represent an unusual system state for the inshore region, driven by intense thermal stratification and suppressed nutrient upwelling in 2014 (Bond et al. 2015, Kintisch 2015, Zaba & Rudnick 2016). We thus contrast 3 ecological scenarios: (1) a relatively typical offshore region, with low productivity, steady-state abundances and Alphaproteobacteria dominance; (2) an unbalanced high-upwelling scenario for the inshore region, with high production and Bacteriodes/Flavobacteria dominance; and (3) a balanced low-upwelling inshore scenario, possibly indicative of a future warmer and strongly stratified ocean, with intermediate productivity and mixed dominance (Fig. 2, Table 1).

Previous studies of taxon-specific bacterial growth rates tend to show very substantial net growth rates in unmanipulated seawater controls over the course of incubations that last 2 to several days. Ferrera et al. (2011), for example, reported net growth rates of 0.4–0.7 d $^{-1}$ for the eubacteria community in seawater control samples from the coastal NW Mediterranean Sea, and net growth rates of up to 1.6–2.3 d $^{-1}$ for the fas-

test growing taxa. For water samples from the same location, Sánchez et al. (2017) found net growth rates of 0.2-0.3 d⁻¹ for the full eubacteria community and 0.5-1.0 d⁻¹ for specific taxa, including SAR11, Rhodobacteria and Gammaproteobacteria. More recently, Fecskeová et al. (2021) determined mean net growth estimates of 0.76 d⁻¹ (range: $0.18-1.79 d^{-1}$) for > 140 OTUs in control samples from the coastal Adriatic Sea. Such estimates greatly exceed the field-validated net growth rates in the present study and suggest unresolved enrichment issues, which could arise from organic release during sample handling and prescreening (Fuhrman & Bell 1985) or incubation conditions that allow phytoplankton blooms (light) or organic decay (dark) over extended experimental durations.

4.5. Growth rate interpretations

Similar to net growth rate estimates, growth rates of bacteria taxa from multi-day dilution cultures or where grazers are filter removed also tend to be high relative to the present results. Fuchs et al. (2000), for instance, reported growth rates from coastal UK waters and the English Channel ranging from 3.2 to $3.8 \,\mathrm{d^{-1}}$ for the bacterial community and 1.0 to 5.1 $\mathrm{d^{-1}}$ for specific taxa. Growth estimates for Proteobacteria and Flavobacteria ranged up to 2.1-5.5 d⁻¹ in dilution cultures conducted with water from the Delaware River estuary (Yokokawa et al. 2004) and up to 3.1 to 4.2 d⁻¹ in Sagami and Otsuchi Bays in Japan (Yokokawa and Nagata 2005). On average, growth rates in 1.0-µm filtered treatments were approximately 2- to 3-fold greater than control net growth rates for most groups investigated by Ferrera et al. (2011) and Sánchez et al. (2017, 2020). The mean growth rate (1.57 d^{-1} ; range: $0.44-5.70 \text{ d}^{-1}$) was also double the control net rate for the numerous OTUs investigated by Fecskeová et al. (2021). In comparison, mean community rates in the present study were below 0.5 d⁻¹ for both inshore and offshore areas in 2014, and only exceeded 1.0 d^{-1} for some taxa during strong upwelling conditions with exceptionally high primary production (Figs. 3 & 4). Given that the commonly used filters (GF/F, 1-µm membrane) to remove or dilute grazers in manipulation studies have the largest effects on dissolved organic carbon enrichment (Fuhrman & Bell 1985), we suggest that the very high growth estimates from such studies might arise from enrichment artifacts.

Among the taxa examined in the 3 CCE ecological scenarios, almost all growth rates (except Verrucomicrobia) were lowest on average in the offshore. Most

also increased over the >30-fold productivity range up to upwelling, though some Flavobacteria (Formosa, NS5, NS2b, Polaribacteria) showed higher mean values at intermediate inshore production. Growth conditions for Flavobacteria taxa and Rhodobacteria were especially poor (below community mean rates) in the offshore region, with the growth rate increases for both groups occurring in parallel with their rising abundances in more productive waters (Figs. 4-6). Conversely, growth rates of Alphaproteobacteria generally and SAR11 and SAR116 in particular were above average in offshore waters, where Alphaproteobacteria predominated, but were also among the highest in active upwelling waters, where their cell concentrations and relative abundances were in significant decline (Figs. 5 & 6). These divergent outcomes imply that the net dynamics of bacterial populations during bloom perturbations are driven more by variability (selectivity) in mortality loss processes than by population differences in growth rates.

While the general magnitude of bacterial community growth rates in the CCE system is grounded in the compatibility of ³H-leucine and FCM dilution results (Landry et al. 2023), population-specific rates are largely unconstrained by independent measurements or by the large ranges of previous literature determinations. Taking the rates at face value, the zero growth rate of Bacteriodes/Flavobacteria in the offshore is suspiciously low, but might be explained by viral decline of some taxa, such as Formosa, while other taxa were growing positively (Fig. 5). Growth rate increases with productivity are consistent with the association of Bacteriodes/Flavobacteria with phytoplankton blooms and richer organic environments (Riemann et al. 2000, Teira et al. 2008) and the lifestyle versatility of Rhodobacterales (Newton et al. 2010). While higher-than-average growth rates of SAR11 are not expected from results of most studies (e.g. Rappé et al. 2002, Ferrera et al. 2011, Sánchez et al. 2017), they are not ruled out by others. For example, Fecskeová et al. (2021) found that SAR11 and SAR116 had high net growth in the Adriatic Sea, with SAR11 (0.97 \pm 0.09 d⁻¹) exceeding both Flavobacteria (0.74 \pm 0.03 d⁻¹) and Rhodobacteria (0.55 \pm 0.05 d⁻¹). Using 16S rRNA to rDNA ratios as a growth rate index, Campbell et al. (2011) also reported substantial variability among SAR11 clades in Delaware coastal waters, with half associated with low growth and half with higher than average growth, and with Flavobacteriaceae showing lower growth ratios than other groups.

However, the same results can also be viewed through the lens of potential bias. For example, since SAR11 is a relatively small cell (Rappé et al. 2002),

their over-representation in filtrate water could have the consequence of exaggerating their growth rate estimates relative to taxa with larger cell sizes. To evaluate the extent to which filtrate artifacts might impact our growth rate conclusions, we recalculated rates for Flavobacteria and SAR11 assuming no filtrate presence for Flavobacteria (i.e. too large to pass the filter) to maximize those rates and assuming 2× overrepresentation of SAR11in the filtrate to minimize those rates. On average, these assumptions increased growth rates of Bacteriodes/Flavobacteria and individual Flavobacteria taxa by $0.09 \pm 0.003 \,\mathrm{d}^{-1}$, and SAR11 rates declined by $0.03 \, d^{-1}$. The net effect of a filtrate artifact is therefore quite modest. Flavobacteria growth rates become more positive, with the highest proportional increase in the offshore, but they are still below average in the offshore and upwelling scenarios, where SAR11 rates remain above average.

PCR bias and 16S copy number variability are more difficult to dismiss as potential artifacts affecting rate calculations, but the present analyses help to constrain those problems to manageable testable hypotheses. For example, because diluted treatments were amplified at least one step more than undiluted treatments in our analyses (to give similar sequence reads for samples with lower absolute concentrations), SAR11 sequences would need to be systematically and significantly amplified relative to Flavobacteria in order to explain high growth rate estimates for SAR11 and low rates for Flavobacteria as a PCR bias. Consistent with that hypothesis, Cottrell & Kirchman (2000) observed that sequence reads substantially overestimate contributions of Alphaproteobacteria and underestimate the Cytophaga - Flavobacter group compared to cell counts by FISH in coastal California waters. As noted previously, Silverman et al. (2021) describe a straightforward approach to test for such an effect, and to mitigate the bias should it be confirmed.

Regarding potential biasing due to 16S copy number, the close agreement between net growth rate estimates from our bottle experiments (derived from initial field-collected samples and unmanipulated seawater after 24 h of *in situ* incubation) and net growth rate estimates for the ambient environment (derived from field-collected samples on successive days) is a strong argument that copy number variability did not significantly or systematically alter the dynamics of populations in the unmanipulated seawater controls. This leaves the dilution treatment as the logical source of an altered copy-number issue, if one exists. To explain high growth rates of SAR11 as a 16S copy artifact, cell copy number would need to increase substantially in the dilution treatment only (e.g. doubling

if the rates are perceived to be 2× too high), and the effect would need to occur broadly from offshore waters, where SAR11 predominates, to upwelling waters, where its abundances are low. Conversely, significant underestimation of Flavobacteria growth rate as a gene copy artifact would imply a dramatic reduction in mean cell copy number over 24 h. Absent other indications of substantial changes in community composition in our dilution treatments, it is unclear what mechanism would select for and drive such abrupt alterations of gene structure. If present, however, it should be revealed by comparisons of taxon contributions to sequence frequencies and FISH cell counts in dilution treatments before and after the 24-h incubations.

5. CONCLUSIONS

Determining group-specific growth rates of HBact in marine systems remains a challenging undertaking, with most manipulation experiments giving net growth estimates that do not reflect the generally observed steady-state abundances of bacteria in natural waters. Following marked water patches in the CCE, we found close agreement between net growth rate estimates from in situ incubations of dilution experiments and community changes in the ambient environment. Net community rates were close to zero in oligotrophic offshore and upwelling-suppressed inshore sites sampled during 2014 heat wave conditions, and sequence-based results for different taxa showed similar magnitudes and positive/negative directional changes between incubation bottles and mixed-layer samples during an upwelling bloom. Using FCM estimates of total HBact to partition relative sequence-based abundances among bacterial taxa, we would rate the resulting determinations of taxon-specific growth rates from 2-treatment dilution experiments as a mixed success. Estimates fall within the poorly constrained results of previous studies and increase with productivity as expected for most groups. However, rate variability is 2 to several times higher than estimates from FCM, and certain taxa, such as SAR11, show higher growth rates than expected relative to the community average. Rate biasing due to disproportionate taxon representation in seawater filtrate did not appear to be of sufficient magnitude to explain high growth of SAR11 in the present experiments, but needs to be explored in more detail. We especially highlight the need to account for possible PCR bias or 16S copy number artifacts in further applications of this approach.

Acknowledgements. This study was supported by US National Science Foundation grant OCE 10-26607 to the CCE LTER Program and by a Scripps Institution of Oceanography Mullin Fellowship to A.L.F. for molecular sample analyses. We thank captains and crews of R/Vs 'Melville', 'Knorr' and 'Thompson' as well as numerous cruise participants for their many contributions to the success of CCE Process cruises. We specifically acknowledge Ralf Goericke, Megan Roadman and Shonna Dovel for cruise chlorophyll, nutrient and primary production data, Mike Stukel and Andrew Taylor for coordinating the drifter array studies, Karen Selph for flow cytometry analyses, John McCrow, Karen Beeri and Hong Zheng for their expertise and help with sequencing and sample processing, and Andrés Gutiérrez-Rodríguez for comments on data analysis.

LITERATURE CITED

- Acinas SG, Sarma-Rupavtarm R, Klepac-Ceraj V, Polz MF (2005) PCR-induced sequence artifacts and bias: insights from comparison of two 16S rRNA clone libraries constructed from the same sample. Appl Environ Microbiol 71:8966–8969
- Alonso-Sáez L, Pinhassi J, Pernthaler P, Gasol JM (2010) Leucine-to-carbon empirical conversion factor experiments: does bacterial community structure have an influence? Environ Microbiol 12:2988–2997
- Baudoux AC, Veldhuis MJW, Noordeloos AAM, van Noort G, Brussaard CPD (2008) Estimates of virus- vs. grazing induced mortality of picophytoplankton in the North Sea during summer. Aquat Microb Ecol 52:69—82
- Bennke CM, Reintjes G, Schattenhofer M, Ellrott A, Wulf J, Zeder M, Fuch BM (2016) Modification of a high-throughput automatic microbial cell enumeration system for shipboard analyses. Appl Environ Microbiol 82: 3289–3296
- Bond NA, Cronin MF, Freeland H, Mantua N (2015) Causes and impacts of the 2014 warm anomaly in the NE Pacific. Geophys Res Lett 42:3414—3420
- Campbell BJ, Yu L, Heidelberg JF, Kirchman DL (2011)
 Activity of abundant and rare bacteria in a coastal ocean.
 Proc Natl Acad Sci USA 108:12,776—12,781
- Chen B (2015) Assessing the accuracy of the 'two-point' dilution technique. Limnol Oceanogr Methods 13:521–526
- Cottrell MT, Kirchman DL (2000) Community composition of marine bacterioplankton determined by 16S rRNA gene clone libraries and fluorescence *in situ* hybridization. Appl Environ Microbiol 66:5116–5122
- Decelle J, Romac S, Stern RF, Bendif EM and others (2015)
 PhytoREF: a reference database of the plastidial 16S
 rRNA gene of photosynthetic eukaryotes with curated
 taxonomy. Mol Ecol Resour 15:1435—1445
- Edgar RC (2010) Search and clustering orders of magnitude faster than BLAST. Bioinformatics 26:2460—2461
- Fecskeová LK, Piwosz K, Šantic D, Šestanovic S and others (2021) Lineage-specific growth curves document large differences in response of individual groups of marine bacteria to the top-down and bottom-up controls. mSystems 6:e00934-21
- Ferrera I, Gasol JM, Sebastián M, Hojerová E, Koblízek M (2011) Comparison of growth rates of aerobic anoxygenic phototrophic bacteria and other bacterioplankton groups in coastal Mediterranean waters. Appl Environ Microbiol 77:7451–7458

- Fuchs BM, Zubkov MV, Sahm KMV, Burkill PHK, Amann R (2000) Changes in community composition during dilution cultures of marine bacterioplankton as assessed by flow cytometry and molecular biological techniques. Environ Microbiol 2:191–201
- Fuhrman JA, Bell TM (1985) Biological considerations in the measurement of dissolved free amino acids in seawater and implications for chemical and microbiological studies.

 Mar Ecol Prog Ser 25:13–21
- Gallegos CL (1989) Microzooplankton grazing on phytoplankton in the Rhode River, Maryland: nonlinear feeding kinetics. Mar Ecol Prog Ser 57:23—33
- Gattuso JP, Peduzzi S, Pizay MD, Tonolla M (2002) Changes in freshwater bacterial community composition during measurements of microbial and community respiration. J Plankton Res 24:1197—1206
- Hammes F, Vital M, Egli T (2010) Critical evaluation of the volumetric 'bottle effect' on microbial batch growth. Appl Environ Microbiol 76:1278—1281
- Jacox MG, Hazen EL, Zaba KD, Rudnick DL, Edwards CA, Moore AM, Bograd SJ (2016) Impacts of the 2015–2016 El Niño on the California Current System: early assessment and comparison to past events. Geophys Res Lett 43:7072–7080
- Kahru M, Jacox MG, Ohman MD (2018) CCE1: Decrease in the frequency of oceanic fronts and surface chlorophyll concentration in the California Current System during the 2014–2016 northeast Pacific warm anomalies. Deep Sea Res I 140:4–13
- Kintisch E (2015) 'The Blob' invades Pacific, flummoxing climate experts. Science 348:17—18
- Kirchman DL (2016) Growth rates of microbes in the oceans. Annu Rev Mar Sci 8:285—309
 - Kirchman DL, Ducklow HW (1993) Estimating conversion factors for the thymidine and leucine method for measuring bacterial production. In: Kemp PF, Sherr BF, Sherr EB, Cole JJ (eds) Handbook of methods in aquatic microbial ecology. Lewis Publishers, Boca Raton, FL, p 513–519
 - Landry MR (1993) Estimating rates of growth and grazing mortality of photoautotrophic plankton by dilution. In: Kemp PF, Sherr BF, Sherr EB, Cole JJ (eds) Handbook of methods in aquatic microbial ecology. Lewis Publishers, Boca Raton, FL, p 715–722
- Landry MR, Hassett R (1982) Estimating the grazing impact of marine micro-zooplankton. Mar Biol 67:283—288
- Landry MR, Brown SL, Campbell L, Constantinou J, Liu H (1998) Spatial patterns in phytoplankton growth and microzooplankton grazing in the Arabian Sea during monsoon forcing. Deep Sea Res II 45:2353–2368
- Landry MR, Brown SL, Rii YM, Selph KE, Bidigare RR, Yang EJ, Simmons MP (2008) Depth-stratified phytoplankton dynamics in Cyclone Opal, an subtropical mesoscale eddy. Deep Sea Res II 55:1348–1359
- Landry MR, Ohman MD, Goericke R, Stukel MR, Tsyrklevich K (2009) Lagrangian studies of phytoplankton growth and grazing relationships in a coastal upwelling ecosystem off Southern California. Prog Oceanogr 83: 208–216
- Landry MR, Selph KE, Taylor AG, Décima M, Balch WM, Bidigare RR (2011) Phytoplankton growth, grazing and production balances in the HNLC equatorial Pacific. Deep Sea Res II 58:524—535
- Landry MR, Selph KE, Stukel MR, Swalethorp R, Kelly TB, Beatty J, Quackenbush CR (2022) Microbial food web

- dynamics in the oceanic Gulf of Mexico. J Plankton Res 44.638-655
- Landry MR, Rivera SR, Stukel MR, Selph KE (2023) Comparison of bacterial carbon production estimates from dilution and ³H-leucine methods across a strong gradient in ocean productivity. Limnol Oceanogr Methods 21: 295–306
- Lessard EJ, Murrell MC (1998) Microzooplankton herbivory and phytoplankton growth in the northwestern Sargasso Sea. Aquat Microb Ecol 16:173—188
- Louca S, Doebeli M, Parfrey LW (2018) Correcting for 16S rRNA gene copy numbers in microbiome surveys remains an unsolved problem. Microbiome 6:1–12
- Mahé F, Rognes T, Quince C, de Vargas C, Dunthorn M (2014) Swarm: robust and fast clustering method for amplicon-based studies. PeerJ 2:e593
- Massana R, Pedrós-Alió C, Casamayor EO, Gasol JM (2001) Changes in marine bacterioplankton phylogenetic composition during incubations designed to measure biogeochemically significant parameters. Limnol Oceanogr 46: 1181–1188
- Monger BC, Landry MR (1993) Flow cytometric analysis of marine bacteria with Hoechst 33342. Appl Environ Microbiol 59:905—911
- Newton RJ, Griffin LE, Bowles KM, Meile C, and others (2010) Genome characteristics of a generalist marine bacterial lineage. ISME J 4:784—798
- Parada AE, Needham DM, Fuhrman JA (2016) Every base matters: assessing small subunit rRNA primers for marine microbiomes with mock communities, time series and global field samples. Environ Microbiol 18:1403—1414
- Pasulka AL, Samo TJ, Landry MR (2015) Grazer and viral impacts on microbial growth and mortality in the southern California Current Ecosystem. J Plankton Res 37: 320–336
- Pearson WR (2016) Finding protein and nucleotide similarities with FASTA. Curr Protoc Bioinformatics 53
- Popendorf KJ, Koblížek M, Van Mooy BAS (2020) Phospholipid turnover rates suggest that bacterial community growth rates in the open ocean are systematically underestimated. Limnol Oceanogr 65:1876—1890
- Quast C, Pruesse E, Yilmaz P, Gerken J and others (2012) The SILVA ribosomal RNA gene database project: improved data processing and web-based tools. Nucleic Acids Res 41:D590—D596
- Rappé MS, Connon SA, Vergin KL, Giovannoni SJ (2002) Cultivation of the ubiquitous SAR11 marine bacterioplankton clade. Nature 418:630–633
- Riemann L, Steward GF, Azam F (2000) Dynamics of bacterial community composition and activity during a mesocosm diatom bloom. Appl Environ Microbiol 66:578—587
- Sánchez O, Michal Koblízek M, Gasol JM, Ferrera I (2017) Effects of grazing, phosphorus and light on the growth rates of major bacterioplankton taxa in the coastal NW Mediterranean. Environ Microbiol Rep 9:300—309
- Sánchez O, Ferrera I, Isabel Mabrito I, Gazulla CR and others (2020) Seasonal impact of grazing, viral mortality, resource availability and light on the group-specific growth rates of coastal Mediterranean bacterioplankton. Sci Rep 10:19773
- Silverman JD, Bloom RJ, Jiang S, Durand HK, Dallow E,

- Mukherjee S, David LA (2021) Measuring and mitigating PCR bias in microbiota datasets. PLOS Comput Biol 17: e1009113
- Stoddard SF, Smith BJ, Hein R, Roller BRK, Schmidt TM (2015) rrnDB: improved tools for interpreting rRNA gene abundance in bacteria and archaea and a new foundation for future development. Nucleic Acids Res 43: D593–D598
- Suzuki MT, Giovannoni SJ (1996) Bias caused by template annealing in the amplification of mixtures of 16S rRNA genes by PCR. Appl Environ Microbiol 62:625–630
- Teira E, Gasol JM, Aranguren-Gassis M, Fernández A, González J, Lekunberri I, Álvarez-Salgado XA (2008) Linkages between bacterioplankton community composition, heterotrophic carbon cycling and environmental conditions in a highly dynamic coastal ecosystem. Environ Microbiol 10:906—917
- Teira E, Martínez-García S, Lønborg C, Álvarez-Salgado XA (2009) Growth rates of different phylogenetic bacterio-

Editorial responsibility: Curtis Suttle, Vancouver, British Columbia, Canada

Reviewed by: K. X. Zhong and 2 anonymous referees

- plankton groups in a coastal upwelling system. Environ Microbiol Rep 1:545–554
- Yokokawa T, Nagata T (2005) Growth and grazing mortality rates of phylogenetic groups of bacterioplankton in coastal marine environments. Appl Environ Microbiol 71: 6799–6807
- Fyokokawa T, Nagata T, Cottrell MT, Kirchman DL (2004) Growth rate of the major phylogenetic bacterial groups in the Delaware estuary. Limnol Oceanogr 49:1620–1629
- Zaba KD, Rudnick DL (2016) The 2014–2015 warming anomaly in the Southern California Current System observed by underwater gliders. Geophys Res Lett 43: 1241–1248
- Zhang J, Kobert K, Flouri T, Stamatakis A (2014) Pear: a fast and accurate Illumina Paired-End reAd mergeR. Bioinformatics 30:614–620
- Zhong KX, Wirth JF, Chan AM, Suttle CA (2023) Mortality by ribosomal sequencing (MoRS) provides a window into taxon-specific cell lysis. ISMEJ 17:105—116

Submitted: July 17, 2023 Accepted: January 2, 2024

Proofs received from author(s): February 25, 2024